Supporting Information

SI Materials and Methods

Proteomics Sample preparation. UTI89 and UTI89Δ*qseC* cultures were grown statically in LB, at 37C for 18h. A total of 4 ml from each culture was pelleted at 6,000rpm for 7 minutes, the cell pellet was solubilized in lysis buffer (Tris-HCl pH 8.5 (30 mM), 7 M urea, 2 M thiourea, and 4% CHAPS), and the total protein content was determined using the Advanced Protein Assay (Cytoskeleton, Inc.). A total pool was generated using equal amounts of each sample to represent all proteins found in the study. An aliquot containing 50 μg of protein from each sample was diluted to 50 μl with lysis buffer (Tris-HCl pH 8.5 (30 mM), 7 M urea, 2 M thiourea, and 4% CHAPS) and labeled with 400 pmol of charge-matched cyanine dyes Cy2, or Cy5 as previously described (Alban *et al.*, 2003). The total pool sample was labeled using Cy3. All labeling reactions were carried out for 45 min at 47˚C, protected from light and quenched with 10 nmol of lysine for 10 min.

2-DE and imaging. Each combined tripartite-labeled sample (450 μl final volume) was rehydrated into 24 cm, 3–10 NL IPG strips (GE Healthcare) under low voltage (100 V) for 12 h, followed by IEF using a Protean IEF cell (Bio-Rad) for a total of 65.5 kVh (using a three-step voltage protocol: 500 V and held for 500 Vh, 1000 V and held for 1000 Vh, 8000 V, and held for 64000 Vh). After focusing, proteins were reduced by placing the IPG strips in 10 ml of equilibration buffer (10 ml, 50 mM Tris (pH 8.8), 6 M urea, 30% glycerol, 2% SDS, bromophenol blue) containing DTT (50 mg) for 15 min at room temperature. The proteins were then alkylated by adding iodoacetamide (600 mg in 10 ml of equilibration buffer). IPG strips were then rinsed with 1X SDS running buffer (25 mM Tris, 192 mM glycine, 0.1% SDS) and layered on 10-20% polyacrylamide gels and sealed with agarose (1% w/v in running buffer).

Commercially prepared gels (Jule, Inc.) were cast between low-fluorescence glass plates using bind-silane (GE Healthcare) to attach the gel to one plate as *per* the manufacturer's instructions. Second-dimension SDS-PAGE separation was carried out on all gels simultaneously using 5 W/gel for the first 15 min followed by 1 W/gel for 17 h with circulating buffer (20°C) in the lower buffer chamber. Images of the labeled proteins in each gel were generated using a Typhoon Imager (GE Healthcare) and the following excitation/emission wavelengths for each dye (488/520 nm for Cy2, 520/580 nm for Cy3, and 620/670 nm for Cy5). After image generation, the gels were fixed (33% ethanol, 7.5% acetic acid) for 2 h, rinsed with deionized water and stored in water-filled, sealed bags at 47˚C.

Gel image analysis and digestion. ImageQuant (Molecular Dynamics) software was used to crop the gel images. The DeCyder (v. 6.5) DIA (difference in-gel analysis) module was used to identify gel feature boundaries and calculate abundance ratios using a normalization algorithm that was applied as previously described (Alban et al., 2003, Karp *et al.*, 2004). Standard parameters were used to determine boundaries estimating 10,000 spots per image. Gel artifacts were removed by software from each gel image using a peak volume filter set at 10,000. Additional gel artifacts (*e.g.* water spots, dust particles) were excluded manually. Images were compared across multiple gels using the DeCyder BVA (Biological Variation Analysis) module. This analysis matched spots in the pool images from each gel, using this sample as a quantitative reference for protein spots in the remaining images allowing quantitative comparison of spots in all images in the experiment. The DeCyder Extended Data Analysis (EDA) module was used to perform t-test analysis. Fifty spots were selected based on their P value (<0.005) and fold change (relative to wt) and excised robotically (ProPic, Genomic Solutions). Proteins in the gel pieces were digested in situ with trypsin (Havlis *et al.*, 2003), and analyzed by mass spectrometry.

Mass Spectrometry Analysis. Samples were processed and analyzed using a nanoflow (200 nl/min) pulse-free liquid chromatograph, interfaced to a quadrupole time-of-flight mass spectrometer (Q-STAR XL, Applied Biosystems) using a PicoView system (New Objective, Woburn, MA), or nano-reversed-phase HPLC interfaced to an electrospray-linear ion trap-Fourier transform ion cyclotron mass spectrometer (LTQ-FT, Thermo-Finnigan) operated as previously described (King *et al.*, 2007). The MS and MS/MS data were collected in the profile mode. The "raw" files were processed using MASCOT Distiller, version 2.1.1.0 (Matrix Science, Oxford, U.K.) and searched using MASCOT version 2.2.04 against the 20080125 Uniprot protein database. The resulting DAT files were imported into Scaffold, ver. 2.02.03 (Proteome Software, Portland, OR) to identify proteins with greater than or equal to 95% confidence and to determine the spectral counts for each protein. An in-house program combined data from MASCOT searches and Scaffold output to generate the peptide tables presented in supplementary data.

Metabolic Phenotype Microarrays. Bacteria from LB agar plates were resuspended into 10 ml of IF-0a GN/GP Base IF (Biolog Inc.) to an 85% transmittance. PM media were prepared according to the manufacturer's instructions, using sodium succinate/ferric citrate as the carbon source for plates PM3-5. Niacin was added to all media (10 µg/ml). Microplates PM1-PM5 (Biolog Inc.) were inoculated with 100 µl of the corresponding PM media containing the bacterial suspension and incubated at 37ºC for 48h (Omnilog Incubator, Biolog). Optical density measurements were obtained at 15 min intervals (OmniLog PM DC 1.30.01 software). Data analysis and kinetic plots generation were performed using OmniLog PM software. Average plot height was used for data comparisons and a difference >20 was set as the significance threshold per the manufacturer's instructions.

Enterobactin quantitation. Enterobactin levels were quantified by liquid chromatography-mass spectrometry (LC-MS) as described by Henderson *et al* (Henderson *et al.*, 2009).

SI Results

Fig. S1 shows the results of microarray and proteome profiling focusing on membrane transport. Fig. S3 shows the different stress response systems the expression of which is altered in the absence of the QseC sensor.

Deletion of *qseC* affects iron homeostasis. Among the dysregulated genes in UTI89Δ*qseC*, 5% are involved in iron homeostasis, including siderophore biosynthesis and transport, transport of free iron, and scavenging of iron from host proteins (Figure 3A, Table SI). Iron is essential for growth and bacteria have developed numerous iron uptake systems to ensure sufficient iron acquisition from diverse environments (Andrews *et al.*, 2003). UTI89 expresses 3 siderophore systems dedicated to the production of yersiniabactin, enterobactin, and salmochelin (Henderson et al., 2009). Previous studies demonstrated that several iron acquisition systems are upregulated in UPEC during infection (Reigstad *et al.*, 2007) and showed a correlation between increased production of yersiniabactin/salmochelin and increased fitness of UPEC during UTI (Henderson et al., 2009).

In contrast to wt UTI89, UTI89Δ*qseC* had increased expression of genes related to enterobactin synthesis (*entBCE* and *entF*) and transport (*fepCG*) (Fig. S2A), suggesting that the siderophore profile of the *qseC* mutant is shifted towards increased enterobactin production. In addition, upregulation of shikimate biosynthetic genes like *aroF* and *pheA* (Geo Accession) also points to increased enterobactin production. We used mass spectrometry to measure enterobactin levels in the supernatants of UTI89 and UTI89Δ*qseC* grown statically over an 18h time course.

This analysis revealed a consistent lag in enterobactin synthesis in UTI89Δ*qseC* during the first 6h of growth (65% reduction) compared to wt UTI89 (Fig. S2B). However, by 18h of growth enterobactin levels in UTI89Δ*qseC* were higher than wt, consistent with the observed upregulation of the corresponding enterobactin biosynthesis genes (Fig. S2B). Thus, deletion of *qseC* dysregulates siderophore expression and could interfere with iron acquisition, influencing other iron import/export systems. Indeed, our analyses showed that ferrous iron importers (*sitABCD*) and hemin uptake systems (*chuAS*, *chuXW*) (Andrews et al., 2003) were upregulated in UTI89Δ*qseC*, whereas, genes associated with iron export (*tsx*, *ompW*) (Lin *et al.*, 2008) were downregulated (Fig. S2A).

Interestingly, the *iscRSUA*, *hscA*, and *fdx* genes (important for generation of [Fe-S] clusters required for the activity of several proteins involved in electron transfer, catalysis and regulatory processes mainly in response to the oxidation status of the cell (Andrews et al., 2003)) were highly upregulated in UTI89Δ*qseC* (Fig. S2A). IscR is an [2Fe-S]-containing regulator (Table SII), which functions as an *iscRSUA* repressor when [Fe-S] clusters exceed the cellular requirements (Andrews et al., 2003). Given that *iscRSUA* expression is elevated, our data indicate that IscR is found in its apo-form, suggesting low [Fe-S] cluster levels. These results indicate that UTI89Δ*qseC* behaves as if it is starved for iron. As iron availability is limited in the host, these impaired responses to iron by UTI89Δ*qseC* argue that a major role of QseBC is to optimize iron acquisition during pathogenesis.

Supplementary Figures and legends

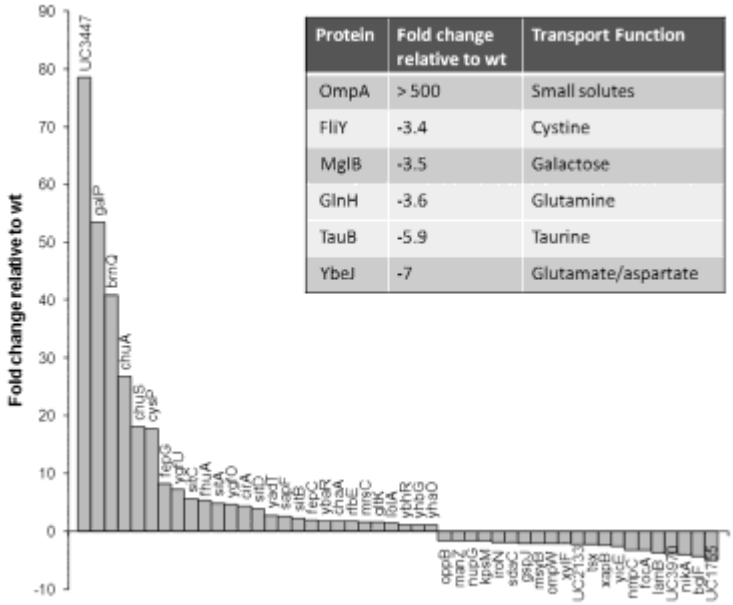

Protein	Fold change relative to wt	Transport Function
OmpA	> 500	Small solutes
FliY	-3.4	Cystine
MglB	-3.5	Galactose
GlnH	-3.6	Glutamine
TauB	-5.9	Taurine
YbeJ	-7	Glutamate/aspartate

Fig. S1. Membrane transporters affected in the *qseC* deletion mutant. Differential expression of factors implicated in membrane transport captured by transcriptional (graph) and proteomics (table inset) analyses.

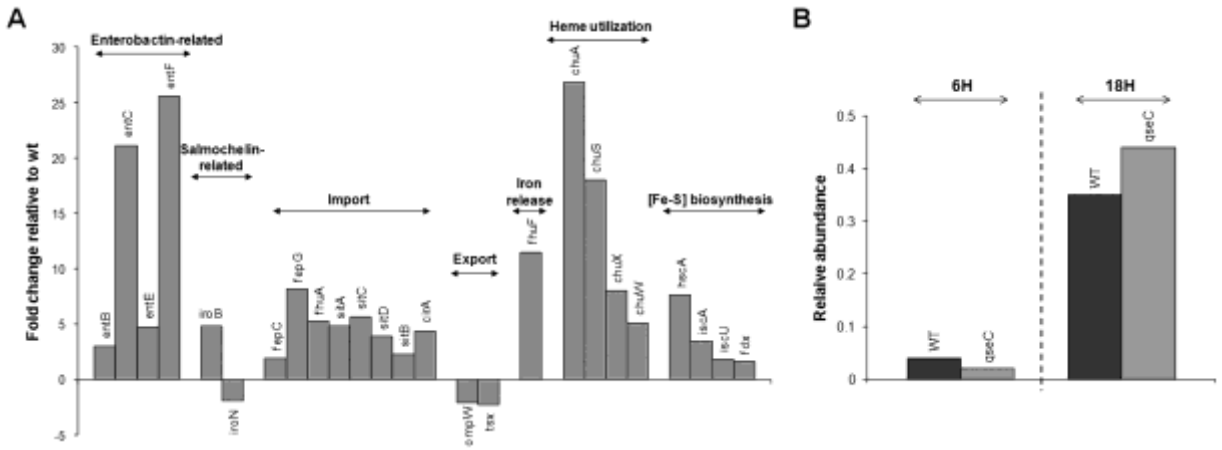

130

131 **Fig S2.** Absence of QseC interferes with iron homeostasis. A) Relative expression patterns of
132 iron-related genes in the *qseC* deletion mutant as determined by microarray. B) Effects of the
133 *qseC* deletion on production of linear enterobactin captured by LC-MS/MS. A representative of 3
134 independent experiments is shown.

135

136

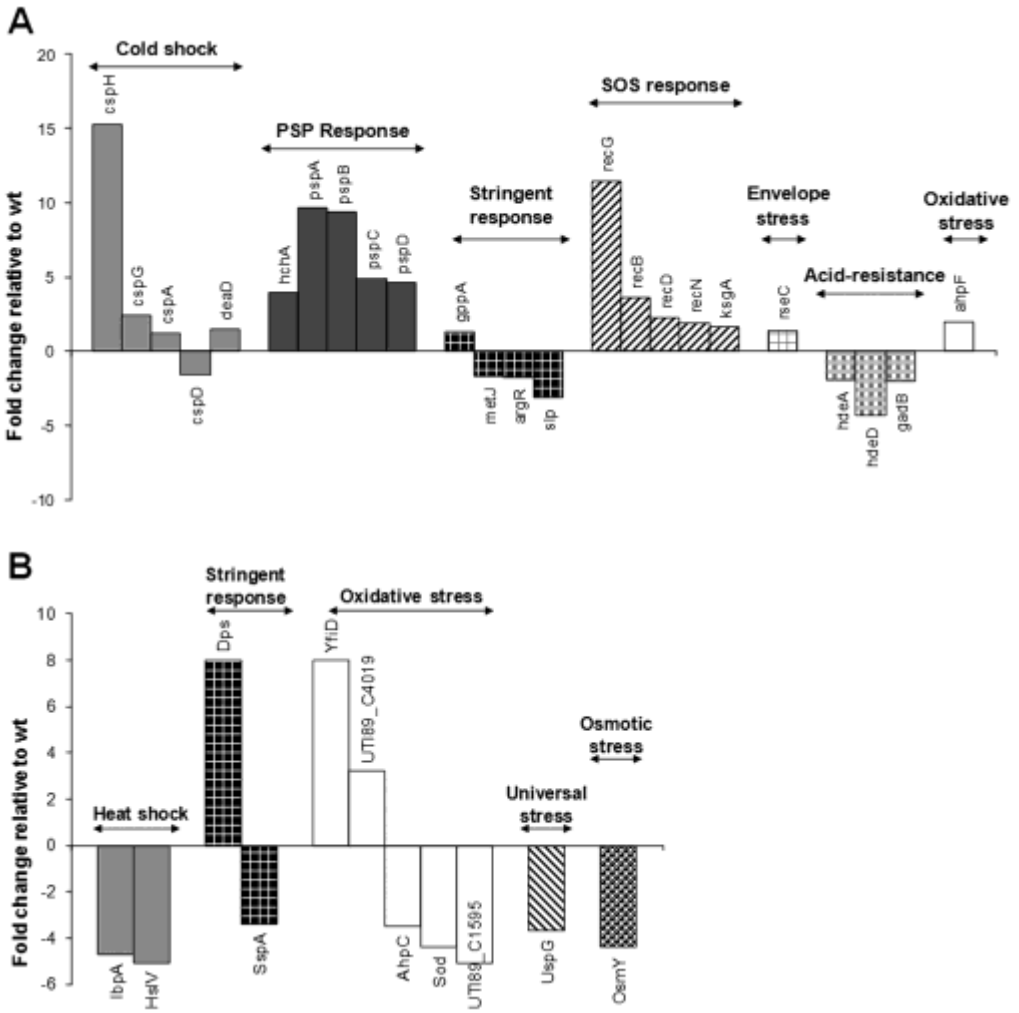

Fig. S3. Stress-responses are dysregulated in the *qseC* deletion mutant. Aberrantly expressed stress-related factors captured by (A) transcriptional and (B) proteomics analyses.

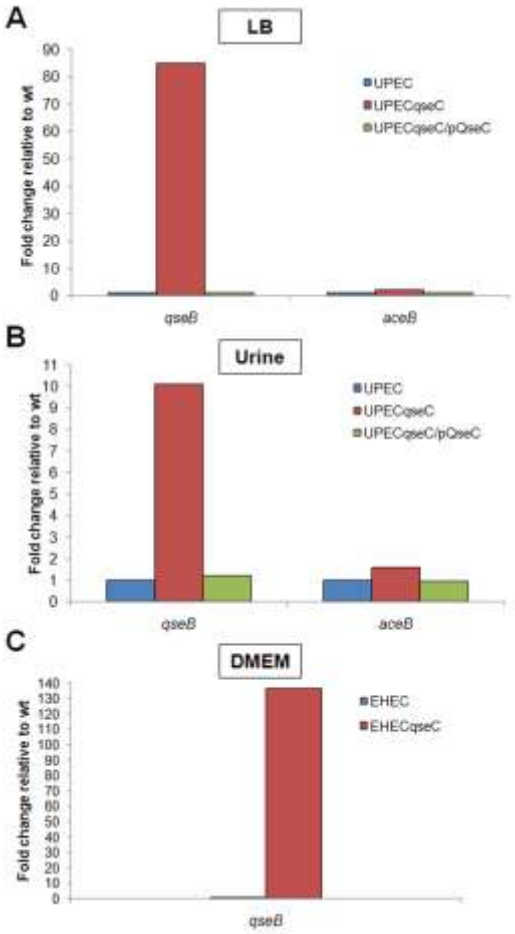

Fig. S4. The gene expression effects upon *qseC* deletion are independent of growth media and conditions. Graphs depicting increased *qseB* and *aceB* expression in: A) UPEC Δ*qseC* grown static in LB media, B) UPEC Δ*qseC* grown static in human urine, and C) EHEC Δ*qseC* grown shaking in DMEM media, as measured by qPCR analyses. Relative fold change was determined by normalizing qPCR values to wt UTI89. A representative of three independent experiments is shown in each panel.

Supplementary Table Titles

Table S1. Transcriptional regulators with altered expression in the absence of QseC

Gene	**Locus**	**Fold-change relative to wt**	**Regulatory function**
Upregulated Targets			
ygiV	UTI89_C3448	527159.23	Hypothetical transcriptional activator
ygiX	UTI89_C3450	531.1	QseB response regulator
pyrI	UTI89_C4850	29.55	Pyrimidine ribonucleotide biosynthesis
sfaB	UTI89_C1108	7.95	S fimbrial switch regulatory protein
phpB	UTI89_C0641	5.33	Putative regulator of metabolism
pspC	UTI89_C1576	4.89	Putative activator of *psp* expression
rstA	UTI89_C1796	2.63	Transcriptional regulator, *csgD* repressor
yfiE	UTI89_C2899	2.61	Hypothetical transcriptional regulator
iscR	UTI89_C2853	2.49	Transcriptional repressor involved in type 1 dependent biofilm formation
yhdM	UTI89_C3737	2.35	Zn(II)-responsive regulator of ZntA
yedW	UTI89_C2168	2.23	Putative TCS response regulator
yhdL	UTI89_C3736	1.92	Putative regulator
yfhA	UTI89_C2873	1.81	QseF response regulator
rseC	UTI89_C2892	1.42	Sigma-E factor regulatory protein RseC
gppA	UTI89_C4333	1.29	Enzyme; global regulatory functions
cspA	UTI89_C4097	1.2	Adaptation to cold-shock
Downregulated targets			
agaR	UTI89_C3560	-1.31	Putative DEOR-type transcriptional regulator of *aga* operon
ymfK	UTI89_C3004	-1.48	Putative phage repressor
ycjZ	UTI89_C0318	-1.49	Hypothetical transcriptional regulator
asnC	UTI89_C4298	-1.57	Asparagine biosynthesis regulator
UC4931	UTI89_C4931	-1.66	Putative response regulator
gntR	UTI89_C3946	-1.7	Regulator of Entner-Douderoff

metJ	UTI89_C4523	-1.72	Methionine biosynthesis regulator
argR	UTI89_C3668	-1.77	Arginine biosynthesis regulator
yedF	UTI89_C2131	-1.89	SirA-like regulator
ygiP	UTI89_C3496	-2.01	Transcriptional activator TtdR
ydjF	UTI89_C1966	-2.22	Putative DEOR-type regulator
UC1288	UTI89_C1288	-2.23	Putative CI repressor of bacteriophage
ybaO	UTI89_C0475	-2.42	Hypothetical transcriptional regulator
yeiL	UTI89_C2437	-2.42	Regulatory protein
xapR	UTI89_C2736	-2.48	Xanthosine operon regulatory protein
ybcM	UTI89_C2134	-2.75	Hypothetical transcriptional regulator
metR	UTI89_C4392	-3.67	Methionine biosynthesis regulator
ybdO	UTI89_C0606	-3.96	Hypothetical transcriptional regulator
sdiA	UTI89_C2117	-3.99	Homolog of quorum sensing regulators
gclR	UTI89_C5031	-4.41	Putative regulator

Table S2. Proteomics raw data and protein identities (provided as a separate Excel spreadsheet).

Table S3. Metabolism-related microarray targets (provided as a separate Excel spreadsheet).

Table S4. Phenotypes gained and lost by EHEC 86-24Δ*qseC* (provided as a separate Excel spreadsheet).

Table S5. Primers used in this study

Primer	**Sequence (5'→3')[1]**	**Description**
MHSH13_Forw	GACTCCTACGGGAGGCAGCA	*rrsh*: 16s rRNA
MHSH14_Rev	CAGCCATGCAGCACCTGTCT	*rrsh*: 16s rRNA
*yehD*_QRT_L	GAGATAATAACCCACGGTATCGTTGC	UTI89_C2385: *yehD* pilin
*yehD*_QRT_R	CTCGACCTATGATGGTGCAGTC	UTI89_C2385: *yehD* pilin
F17-like_QRT_L	TTATTCGTAGGCAATGGTATAATGGACC	UTI89_C4907: F17-like pilin
F17-like_QRT_R	CTTTTGGGGGAAGCGGATAATGGG	UTI89_C4907: F17-like pilin
*rstA*_qPCR_Forw	CTCGATAGCGATATGAACCACATCCTGG	UTI89_C1796: curli regulator

*rstA*_qPCR_Rev	GTAGGGAGTCAGAGACGTTTCCTGAATAC	UTI89_C1796: curli regulator
*csgD*_qPCR_Forw	GTTGTTTTTCCTGCTCAAAGTATCCTGCC	UTI89_C1161: curli regulator
*csgD*_qPCR_Rev	ACTAAACCTTCTTTGCAGGCGACAGCTC	UTI89_C1161: curli regulator
*aceB*_qPCR_Forw	GCGGTCTGCACTTGCCGGAAAAACATG	UTI89_C4573: *aceB* malate synthase
*aceB*_qPCR_Rev	CGCGGCAGATTAAAGCGATCTTCTGC	UTI89_C4573: *aceB* malate synthase

SI References

Alban, A., S. O. David, L. Bjorkesten, C. Andersson, E. Sloge, S. Lewis & I. Currie, (2003) A novel experimental design for comparative two-dimensional gel analysis: two-dimensional difference gel electrophoresis incorporating a pooled internal standard. *Proteomics* **3**: 36-44.

Andrews, S. C., A. K. Robinson & F. Rodriguez-Quinones, (2003) Bacterial iron homeostasis. *FEMS Microbiol Rev* **27**: 215-237.

Havlis, J., H. Thomas, M. Sebela & A. Shevchenko, (2003) Fast-response proteomics by accelerated in-gel digestion of proteins. *Anal Chem* **75**: 1300-1306.

Henderson, J. P., J. R. Crowley, J. S. Pinkner, J. N. Walker, P. Tsukayama, W. E. Stamm, T. M. Hooton & S. J. Hultgren, (2009) Quantitative metabolomics reveals an epigenetic blueprint for iron acquisition in uropathogenic Escherichia coli. *PLoS Pathog* **5**: e1000305.

Karp, N. A., D. P. Kreil & K. S. Lilley, (2004) Determining a significant change in protein expression with DeCyder during a pair-wise comparison using two-dimensional difference gel electrophoresis. *Proteomics* **4**: 1421-1432.

King, J. B., J. Gross, C. M. Lovly, H. Piwnica-Worms & R. R. Townsend, (2007) Identification of protein phosphorylation sites within Ser/Thr-rich cluster domains using site-directed mutagenesis and hybrid linear quadrupole ion trap Fourier transform ion cyclotron resonance mass spectrometry. *Rapid Commun Mass Spectrom* **21**: 3443-3451.

Lin, X. M., L. N. Wu, H. Li, S. Y. Wang & X. X. Peng, (2008) Downregulation of Tsx and OmpW and upregulation of OmpX are required for iron homeostasis in Escherichia coli. *J Proteome Res* **7**: 1235-1243.

Reigstad, C. S., S. J. Hultgren & J. I. Gordon, (2007) Functional genomic studies of uropathogenic Escherichia coli and host urothelial cells when intracellular bacterial communities are assembled. *J Biol Chem* **282**: 21259-21267.